Modern Applications of EPR/ESR

From Biophysics to Materials Science

APS'97

Proceedings of the
First Asia-Pacific EPR/ESR Symposium
Hong Kong
20 – 24 January 1997

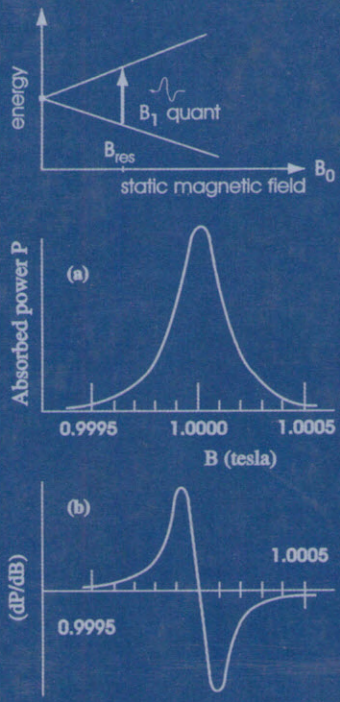

C.Z. Rudowicz
(Editor)

K.N. Yu
H. Hiraoka
(Associate Editors)

Springer

Modern Applications of EPR/ESR

From Biophysics to Materials Science

Proceedings of the
First Asia-Pacific EPR/ESR Symposium
Hong Kong
20 - 24 January 1997

C.Z. Rudowicz
(Editor)

K.N. Yu
H. Hiraoka
(Associate Editors)

Springer

Czeslaw Z. Rudowicz and K.N. Yu
Department of Physics and Materials Science
City University of Hong Kong
Tat Chee Avenue
Kowloon
Hong Kong

H. Hiraoka
Department of Chemisty
Hong Kong University of Science and Technology
Clear Water Bay
Kowloon
Hong Kong

Library of Congress Cataloging-in-Publication Data

Asia-Pacific EPR/ESR Symposium (1st : 1997 : Hong Kong)
Modern applications of EPR/ESR : from biophysics to materials science : proceedings of the the First Asia-Pacific EPR/ESR Symposium, Hong Kong, 20-24 January 1997 / Czeslaw Z. Rudowicz (editor), K.N. Yu, H. Hiraoka (editors).
p. cm.
Includes bibliographical references.
ISBN 9813083239
1. Electron paramagnetic resonance spectroscopy--Congresses.
2. Electron paramagnetic resonance spectroscopy--Industrial applications--Congresses. I. Rudowicz, Czesław. II. Yu, K. N., 1963- . III. Hiraoka, H., 1932- . IV. Title.
QC763.A78 1997
543'.0877--dc21

97-22627
CIP

ISBN 981-3083-23-9

Typesetting: Camera-ready by authors
SPIN 10636243 5 4 3 2 1 0

Conduction ESR and Current Carriers Injection Phenomenon at Incommensurate Crystallization of "Guest" Molecules in Acceptor Graphite Intercalation Compounds

A.M. Ziatdinov and N.M. Mishchenko

Institute of Chemistry, Far-Eastern Division of the RAS, Vladivostok, Russia

Abstract. The investigations of the effect of temperature on the conduction electron spin resonance (CESR) spectra of graphite intercalation compounds (GICs) $C_{10}HNO_3$ were realized with the 2D-CESR line shape analysis procedure developed by the authors. Conductivities along σ_a and perpendicular σ_c to GICs basal planes have also been measured. As a result, we established an earlier unknown phenomenon: when layers of "guest" molecules undergo an aggregate phase transition (at $T_c \sim 250$ K), σ_a and σ_c increase in spite of the decrease of the charge carrier mobility. CESR measurements of charge carrier concentration N vs. temperature show that this unusual "nonmetallic" behavior of GICs results from the increase of the hole concentration in π-bands. The increase of N is directly connected with the partial localization of the conduction π-electrons (in terms of GICs tight binding model). Because the localized electrons are scattering centers for the conduction electrons, the increase in N must obviously be accompanied by a decrease in conduction electron mobility and an increase in CESR line width.

1 Introduction

The temperature dependence of the conduction electron spin resonance (CESR) line width (ΔB) in metals has been successfully explained [1] in terms of the Elliot's theory [2] according to which $\Delta B = \alpha(\Delta g)^2/\tau$, where α is a constant, Δg is the g-shift from the free electron value, and τ is the conductivity relaxation time. The frequency of the electron-electron and electron-phonon collisions decreases with temperature and, as a result, τ increases, while the concentration (N) of the current carriers remains practically constant because of large values of Fermi temperature [3]. As a result, when the temperature lowers, the conductivity of pure metals $\sigma = Ne^2\tau/m^* = Ne\mu$ (m^*, e and μ are the effective mass, charge and mobility of charge carriers, respectively) increases, and simultaneously, if Δg is temperature independent, the CESR line width decreases.

In graphite intercalation compounds (GICs) of the acceptor type $C_{10}HNO_3$ we found a relation between σ and ΔB other than in pure metals. In this synthetic metal during and after intercalate crystallization Δg is

unchanged, while both the electroconductivity and the CESR line width increase simultaneously. In this paper we report the results of an investigation of the CESR line width "nonmetallic" temperature dependence origin in GIC $C_{10}HNO_3$

2 Experimental

GICs comprise a wide class of synthetic metals and consist of an alternating sequence of n hexagonal graphite monolayers (n is the stage index) and a monolayer of "guest" atoms or molecules (intercalate) [4]. The compounds $C_{10}HNO_3$ investigated belong to the second stage of α - modification of GICs with nitric acid of the general formula $C_{5n}HNO_3$ (n = 1, 2, 3,...) [4,5]. According to the data of various physical methods [4], in these GICs the two-dimensional liquid-like layers of HNO_3 are ordered and form a two-dimensional crystal at T≤ 250 K. In $C_{10}HNO_3$ layers of HNO_3 are incommensurable with a carbon net and they undergo a structural phase transition of the incommensurate phase-commensurate phase type at T~210 K [6].

CESR spectra of GIC $C_{10}HNO_3$ plates were registered at X-band (ν=9.5 GHz) in the temperature range 100 ÷ 300 K using the rectangular resonator with the TE_{102} mode and 2.5 kHz modulation of an external constant magnetic field $\mathbf{B}_o$. At the conventional setting of the resonator, the electrical component of the microwave field is parallel to $\mathbf{B}_o$; in the geometric center of the resonator the magnetic component of this field is parallel to the vertical axis of the resonator.

Highly oriented pyrolitic graphite plates required for GIC synthesis were cut out of a single bar with the basal plane conductivity equal to (1.2 ± 0.2)×10^4 $Ohm^{-1}\cdot cm^{-1}$. These plates had a shape of a rectangular parallelepiped with dimensions: width (l) × height (h)× thickness (d), where l×h is the square of a basal plane. Accuracy in determining the size of plates was ~5×10^{-4} cm. Synthesis of GIC $C_{10}HNO_3$ was carried out in nitric acid with the density ρ=1.562 $g\cdot cm^3$. The GIC stage was controlled by the diffraction method. The effect of temperature on CESR line shape parameters was investigated using the plate of size: 0.40×0.40×0.02 cm^3.

3 Results and Discussion

In the entire temperature range of investigations a single asymmetric CESR signal of $C_{10}HNO_3$ is observed. Down to ~ 250 K the asymmetry parameter of the first derivative of the absorption line A/B (which is defined as the ratio of the maximum peak height (A) to the minimum peak height (B), both measured with respect to the zero line of the resonance derivative) and the width of the CESR line at half height of the peak A are independent of

temperature and are equal to 3.0±0.1 and 2.2×10^{-5} T, respectively. At all temperatures, the spectrum is axial with respect to the c- axis and is characterized by $g_{\parallel} = 2.0023 \pm 0.0001$ and $g_{\perp} = 2.0028 \pm 0.0001$. The line width increases as temperature decreases below 250 K (Figs 1 and 2). Simultaneously, the A/B value decreases, and it is equal to 2.6 ± 0.1 at 96 K (Fig. 2). The derivative $d(\Delta B)/dT$ undergoes the step-wise changes at T_{c1}· =250 K, T_{c2}· =249.8 K, T_{c3}· =248 K, T_{c4}· =247 K, T_{c5}· =243 K (Fig 1). As the temperature increases ΔB and A/B values change inversely but with a "global" temperature hysteresis (Figs. 1 and 2). Temperatures T_{ci}· (T_{ci}⁺) (i=1÷5) are close to the temperature of the intercalate crystallization (melting) in $C_{10}HNO_3$ (T_c ~ 250 K) known from literature [4]. This allows us to treat the CESR line shape transformations observed in $C_{10}HNO_3$ at T_{ci}· (T_{ci}⁺) (i=1÷5) as a result of the multi-step change in $C_{10}HNO_3$ the aggregate state of the "guest" molecules. The CESR line shape transformation at T_{ci}*, is probably due to

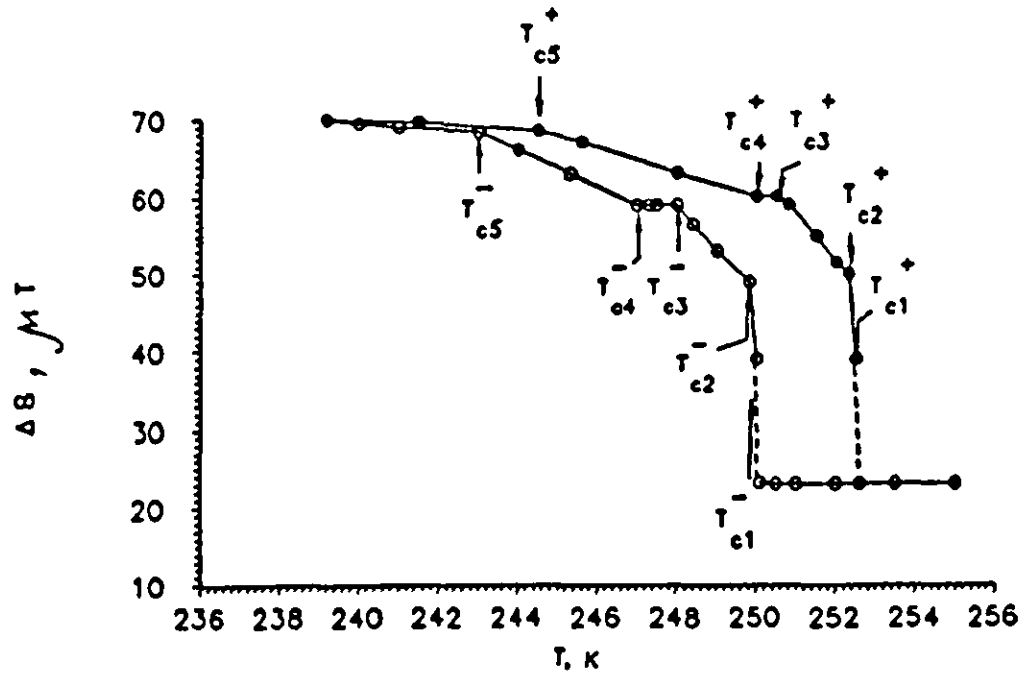

Fig. 1. Temperature dependence of CESR linewidth ΔB of $C_{10}HNO_3$ plate with dimensions: 0.4 × 0.4 × 0.02 cm³ during crystallization (unfilled symbols) and melting (filled symbols) of intercalate. T_{ci}· (T_{ci}⁺) are the temperatures of the step-wise changes of the derivative $d(\Delta B)/dT$ at cooling (heating) of the sample, respectively. $B_o \perp c$, ν = 9.52 GHz.

the incommensurate-commensurate phase transition. At powers of the microwave field far from saturation of the CESR signal and at the same temperature, ΔB values in Q- and X- bands coincide indicating that the CESR line is homogeneously broadened.

The basal plane electroconductivity (σ_a) of $C_{10}HNO_3$ plates was measured by the contactless induction method using a device analogous to that described by Pendrys *et al.* [7]. The results of σ_a measurements are

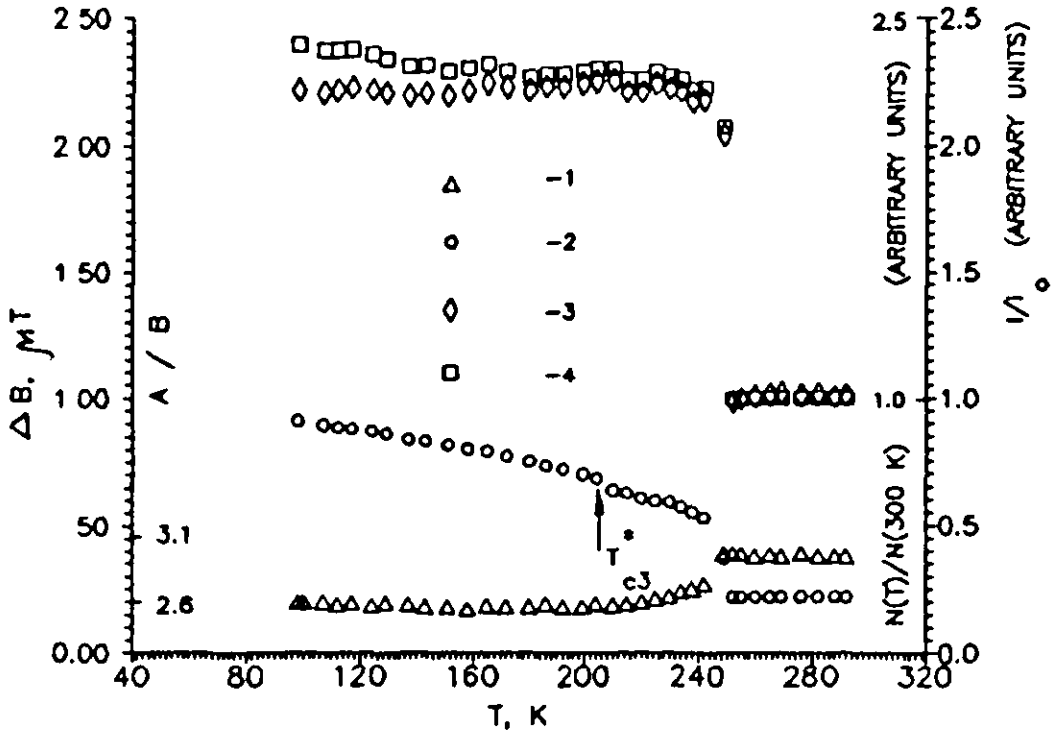

Fig. 2. Temperature dependence of CESR line parameters of $C_{10}HNO_3$ plate with dimensions: 0.4 × 0.4 × 0.02 cm³, i.e., $A/B(T)$ (curve 1), $\Delta B(T)$ (curve 2), $I(T)/I_o$ (curve 3), where $I = (A+B)\,\Delta B^2$ and I_o is the intensity of the Mn^{2+} ESR line in a standard sample ZnS:Mn^{2+}, and the relative spin concentration $N(T)/N(300\ K)$ (curve 4), determined by the expression (1). Unfilled symbols correspond to experimental values of parameters at cooling of the GIC. T_{c3}* is the temperature of the peak of the derivative $d(\Delta B)/dT$. $\mathbf{B}_o \perp \mathbf{c}$, $\nu = 9.52$ GHz.

presented in Fig. 3, and indicate that the σ_a increases as temperature decreases.

In the microwave field of a given configuration only the conduction plate regions adjacent to the vertical faces ($h \times l$) and ($h \times d$), situated approximately within the skin-depth, contribute to the CESR [8,9]. In $C_{10}HNO_3$ one may neglect the contribution to CESR from regions adjacent to the basal planes ($h \times l$) due to the high conduction anisotropy (~ 10^5) [4]. This peculiarity of $C_{10}HNO_3$ plates allows us to analyze their CESR line shape, in particular, at contactless determination of the c-axis electroconductivity (σ_c) (see below), using the one-dimensional Dyson expression [10] for CESR line shape in isotropic metals and well known Feher and Kip [11] or Kodera [12] nomograms calculated on the basis of this expression.

The σ_c measurement is not a trivial problem. The contactless method to determine the σ_c of acceptor GICs was suggested by Saint-Jean and McRae [13]. They recommended the use of the well known A/B vs l/δ_c nomograms [8,9,12,13] at interval $l/\delta_c < 2.5$ for this purpose. At this interval the ratio of A/B does not depend on spin carriers mobility [8,9,12,13]. This enables one to determine the value of δ_c and, consequently, the value of σ_c unambiguously, by measuring the values of A/B and l. However, in narrow

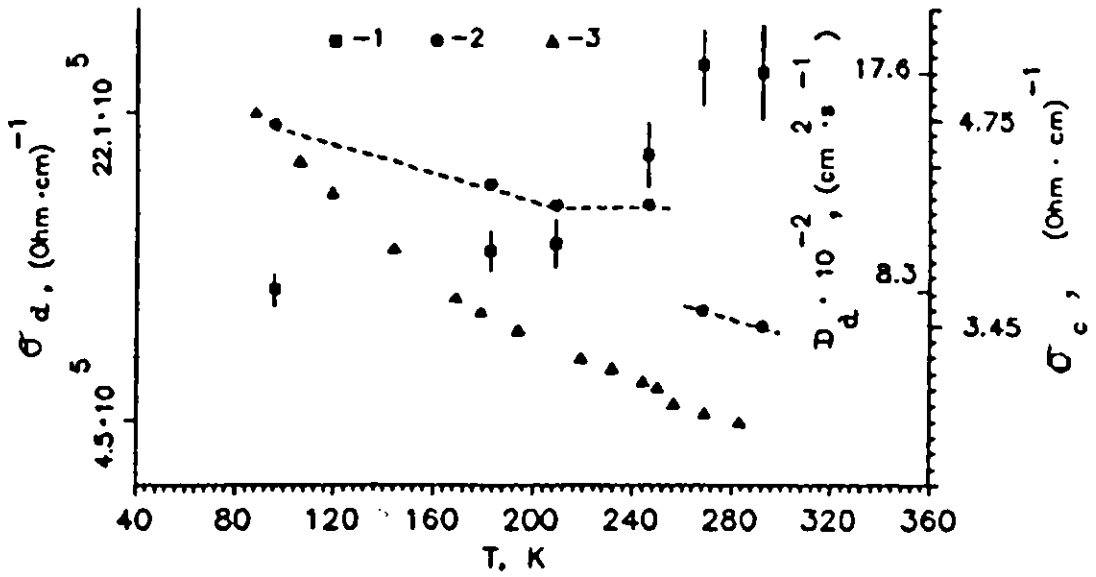

Fig. 3. Temperature dependence of D_d (1), σ_c (2) and σ_d (3) in $C_{10}HNO_3$. The dashed lines correspond to the linear functions σ_c = [(-4.17×10^{-3}/ K)T+ 4.7] (Ohm cm)$^{-1}$, σ_c =4.21 (Ohm cm)$^{-1}$ and σ_c = [(-5.86 ×10^{-3}/ K)T+5.28] (Ohm cm)$^{-1}$ for $T > T_{c1}$, 209 K < T <246 K and 96 K < T < 209, respectively.

samples of GICs with HNO_3 [14] as well as in narrow samples of GICs with AsF_5 [13] the values of σ_c and spin carriers diffusion constant differ from values of this parameters in wide samples. This unusual result for narrow GIC samples is likely connected with the fact that the intercalate layers composition and organization depend on a sample size [14]. That is why another contactless method was used to determine the value of σ_c in our study. The principles of this method are as follows.

It follows from the one-dimensional Dyson expression for CESR line shape in metals [10] that the coordinate of the maximum (l_{max}/δ_c) of the $A/B(l/\delta_c)$ dependence and the value of asymmetry parameter on "plateau" at ($l/\delta_c > 10$) of this dependence [$(A/B)_{plat}$] are unambiguously related to each other. The corresponding nomogram calculated by the authors is presented in Fig.4. The theoretical value of l_{max}/δ_c can be found from this nomogram, if the experimental value of $(A/B)_{plat}$ is known. Then, at a given frequency of the microwave field, the value of σ_c can be easily calculated, if the experimental value of l_{max} is known as well. It must be emphasized that the given procedure of σ_c -determination is applicable only in the case when (1) one may neglect the contribution to CESR from regions adjacent to the basal planes ($h \times l$) of GIC plates and (2) the CESR line shapes of plates with $l \sim l_{max}$ as well as plates with l from "plateau" of the $A/B(l)$ dependence should be described by the one-dimensional Dyson expression for CESR line shape [10] with the same value of σ_c and the in-plane diffusion time across the skin -depth δ_c (T_{Da}) determined by the σ_c .Because of this, before the procedure under consideration

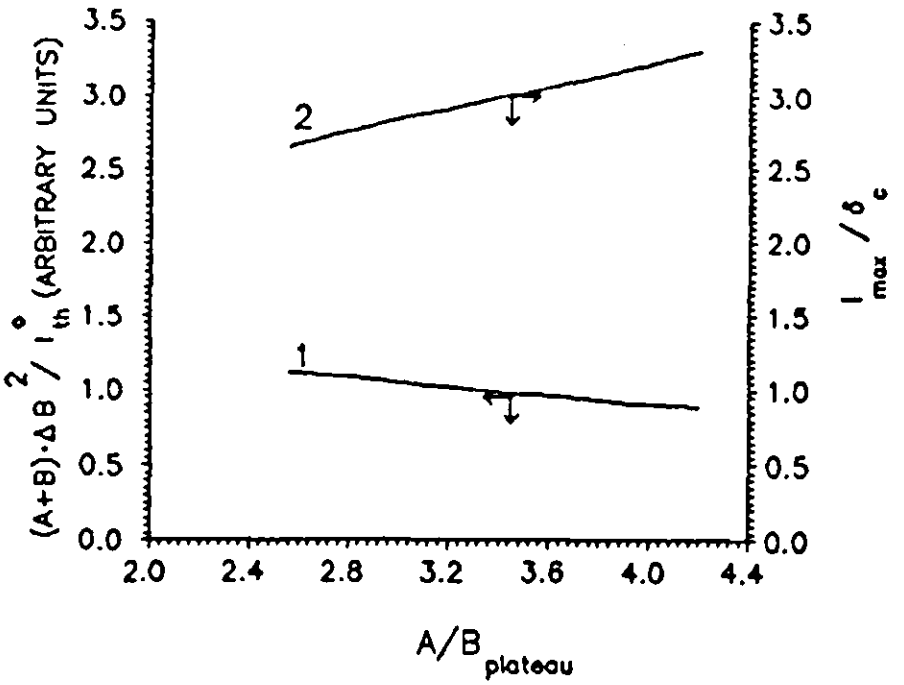

Fig. 4. The relation of theoretical value of intensity $I = (A+B)\cdot\Delta B^2 / I_{th}^{\bullet}$ (curve 1) and coordinate of the maximum (l_{max} / δ_c) of the theoretical dependence $A/B(l / \delta_c)$ (curve 2) plotted against the value of A/B on the "plateau" of the $A/B(l / \delta_c)$ dependence at ($l / \delta_c > 10$). $I_{th}^{\bullet}$ is the value of the I_{th} at A/B = 3.0 (in the quasi-liquid phase of the intercalate).

was applied to determine the σ_c-value in $C_{10}HNO_3$, the experimental $A/B(l)$ dependence was studied in more detail at fixed temperature both before (at 292 K and 268 K) and after (at 246 K, 209K, 183 K and 96 K) the phase transition. Then this dependence was approximated by the corresponding theoretical curve calculated from the one-dimensional Dyson expression for CESR line shape [10] with the value of σ_c determined from the experimental values of l_{max} and $(A/B)_{plat}$ and the value of T_{Da} determined by the standard procedure [11,12] (using the values of ΔB and A/B of GIC plates with l from "plateau" of the $A/B(l)$ dependence). As seen from Fig. 5, the theoretical and experimental dependences $A/B(l)$ are in good agreement at $l > l_{max}$. Taking it into consideration , the values of σ_c at other temperatures were determined using the experimental values of l_{max} and $(A/B)_{plat}$ only. By this procedure of σ_c -determination we established that σ_c, as well as σ_a increases with decreasing the temperature (Fig. 3). Hence in $C_{10}HNO_3$, during and after intercalate crystallization the ΔB increases simultaneously with the conductivity in spite of the fact that the g tensor values of the spin carriers are temperature independent. We have found a possible explanation for this uncommon property of the CESR line width temperature dependence by investigating the temperature effect on N and on the in-plane spin diffusion constant (D_a).

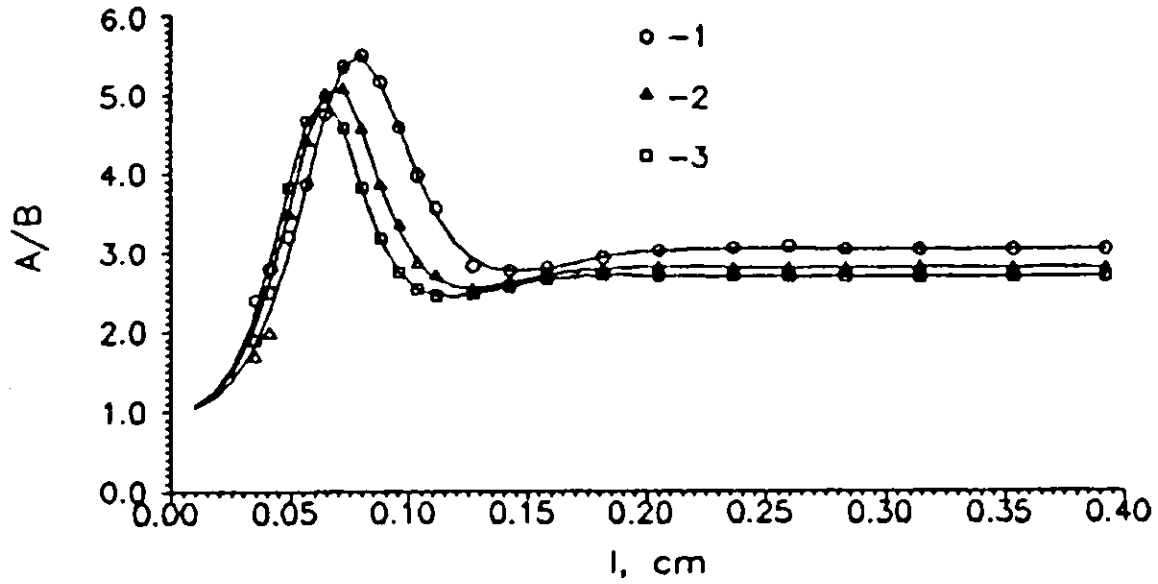

Fig. 5. The experimental (open symbols) and theoretical (solid lines) values of the line asymmetry parameter A/B of the $C_{10}HNO_3$ plates with dimensions $l \times 0.40 \times 0.02$ cm^3 as a function of sample width (l). The experimental curves 1, 2 and 3 correspond to 296 K , 209 K and 96 K, respectively. $\mathbf{B}_0 \perp$ c, ν = 9.52 GHz. The theoretical curves at 296 K, 209 K and 96 K are one-dimensional Dyson's [10] curves with σ_c = 3.45, 4.2 and 4.75 (Ohm cm)$^{-1}$, T_{D_0} = 21.7, 30.5, and 33.5 in the units of 10^{-8} s, respectively.

At a given geometry of the GIC sample the CESR signal integral intensity $I=(A+B)\Delta B^2$ is proportional to $N\delta_c$. Because of this, the increase in I simultaneously with the decrease in δ_c , which takes place in $C_{10}HNO_3$ as the temperature decreases from T_{c1}· to T_{c3}* (Fig. 2), suggests that N increases in this temperature range. This conclusion does not change once the 7.5 % increase of I (relative to its value in liquid phase of intercalate) along with the decrease of A/B at this temperature range has been taken into consideration with the help of the corresponding nomogram in Fig. 4. Further, using the relation $I \sim N\,\delta_c$ and approximating the experimental values of σ_c before and after phase transition by the linear functions (see Fig. 3) we have calculated the temperature dependence of the relative spin carriers concentration (Fig. 2):

$$N(\mathrm{T})/N(300\ \mathrm{K}) = [I(\mathrm{T})/I(300\ \mathrm{K})][\,\sigma_c(\mathrm{T})/\,\sigma_c(300)]^{1/2}, \qquad (1)$$

where N(300 K), I(300 K) and σ_c(300 K) are the values of N, I and σ_c at 300 K, respectively. As should be expected from the results of the qualitative analysis of the experimental data, N increases as the temperature is lowered in the crystal phase of the intercalate (Fig. 2). Concerning the behaviour of N in the quasi-liquid phase of the intercalate, all its variations occur within the experimental error (Fig. 2). It follows from above that in synthetic metal $C_{10}HNO_3$ in the solid phase of the intercalate the increase of σ_c is at least partially due to the increase in N.

With knowledge of the experimental values of A/B and ΔB of GIC plates with l from " plateau " of the $A/B(l)$ dependence and using the Feher and Kip [11] nomograms one can easily determine T_{Da}. According to Dyson [10], in the approximation of independent electrons, the value T_{Da} is connected with the value of D_a by the relationship $D_a = \delta_c^2/2T_{Da}$. The estimation of D_a according to this expression has shown (Fig. 3) that its value during and after intercalate crystallization decreases.

The diffusion constant is equal to

$$D_a = (1/3)\,\Lambda_a v_a = (1/3)\,\tau_a v_a^2 \qquad (2)$$

by definition [3]. In the expression (2) Λ_a, τ_a and v_a are the mean free path, the electroconductivity relaxation time and the spin carriers velocity, all along the basal plane. If in expression (2) v_a is identified with Fermi velocity v_F and it is taken into account that in metals v_F is proportional to the square of current carriers concentration [3] then it may be concluded, from this expression, that τ_a in $C_{10}HNO_3$ decreases during and after intercalate crystallization (since at this process D_a decreases simultaneously with the increase of N). This suggests that "nonmetallic" broadening of the CESR line in $C_{10}HNO_3$ is due to the decrease of the in-plane current carriers mobility.

The broadening of the CESR line is homogeneous. The g-tensor values of spin carriers are independent of the changes in aggregate states of the intercalate and they are close to the g-tensor value of the free electron. These facts testify that the density of charge carriers on intercalate molecules is small and does not change at phase transition. Above, it is shown that it is possible to analyze the transformations of the electronic properties of $C_{10}HNO_3$ induced by phase transition in terms of the rigid electronic band model of GICs [4,15]. In terms of this model, in acceptor GICs related to the conductors with the hole Fermi surface [4] the increase of N as the temperature decreases is possible only at lowering of the Fermi energy, for instance, due to the transfer of the additional electrons from carbon layers to intercalate layers [4,15], or due to the localization of spin carriers in graphite layers, preferentially at the edges of the Dumas-Herold islands [16]. In this case, the increase in N must obviously be accompanied by the decrease in τ_a, and consequently, by the increase in ΔB, because the localized electrons are the perturbation centers for the conduction electrons. That is, in the crystal phase of the "guest" molecules subsystem, the rigid electronic band model predicts qualitatively the correct temperature effect on these experimental values. Note that several recent experimental results confirm the existence in GICs of the localized moments and traps. For instance, Davidov *et al.* [17] observed the presence of localized moments in the graphite layers by spin-echo techniques performed on AsF_5 GICs and suggested the existence of traps. A precise analysis of the spin-relaxation time [13] and the anisotropy of the line width with the orientation of $\mathbf{B}_0$ [18] confirms this assumption. At the present time, the exact nature of these traps remains to be determined.

Acknowledgments

This work was supported by Russian Foundation for Basic Research grant (N 97-03-33346 a). The authors are grateful to L.B. Nepomnyashchii (State Research Institute of Graphite, Moscow) for the HOPG plates used in the synthesis of GIC.

References

1 P. Monod and F. Beuneu, Conduction electron spin flip by phonons in metals: Analysis of experimental data, *Phys.Rev.B* 19, 12 (1979) 911-916.
2. R.J. Elliot, Theory of the effect of spin-orbit coupling on magnetic resonance in some semiconductors, *Phys.Rev.* 96 (1954) 266.
3. N.W. Ashcroft and D. Mermin, Solid State Physics, Cornel University, Holt, Rinehard and Winston, N.Y. (1976).
4. M.S. Dresselhaus and G. Dresselhaus, Intercalation compounds of graphite, *Adv.Phys.* 30 (1981) 139.
5. M.J. Bottomly, G.S. Parry and A.R. Ubbelohde, Thermal expansion of some salts of graphite, *Proc.R.Soc.London* A279, 1378 (1964) 291-301.
6. F. Batallan, I. Rosenman, A. Magerl and H. Fuzellier, Two-dimensional molecular diffusion and phase transition in HNO_3 - intercalated graphite studied by quasielastic neutron scattering, *Phys.Rev.B* 32 (1985) 4810.
7. L.A. Pendrys, C. Zeller and F.L. Vogel, Electrical transport properties of natural and synthetic graphite, *J.Mat.Sci.* 15, 11 (1980) 2103-2112.
8. A.M. Ziatdinov and N.M. Mishchenko, Electron spin resonance line shape and kinetic parameters of the conduction electrons in highly anisotropic conductors: highly oriented pyrolytic graphite *Phys. Solid State*, 36, 8 (1994) 1280-1289.
9. J. Blinowski, P. Kacman, C. Rigaux and M. Saint-Jean, Effect of conduction anisotropy of GIC on ESR line shape. *Synth.Met.* 12 (1985) 419-423.
10. F.J. Dyson, Electron spin resonance absorption in metals. II. Theory of electron diffusion and the skin effect. *Phys.Rev.* 98 (1955) 349-359.
11. G. Feher and A.F. Kip, Electron spin resonance absorption in metals I. Experimental *Phys.Rev.* 98, 2 (1955) 337-348.
12. H. Kodera , Dyson effect in the electron spin resonance of phosphorus doped silicon, *J.Phys.Soc.Jpn.* 28, 1, (1970) 89-98.
13. M. Saint-Jean and E. McRae, Planar diffusion constant D_a in acceptor graphite intercalation compounds, *Phys.Rev.* 43, 5 (1991) 3969-3974.
14. A.M. Ziatdinov and N.M. Mishchenko, unpublished data.
15. S.Y. Leung and G. Dresselhaus, Dispersion relations in graphite intercalation compounds: Electronic energy band, *Phys.Rev.B* 24 (1981) 3490-3504.
16. A.M. Ziatdinov, N.M. Mishchenko and Yu.M. Nikolenko, Phase transitions and incommensurate states in GIC C_{5n} HNO_3, *Synth.Met.* 59, 2 (1993) 253-258.
17. D. Davidov, A. Grupp, H. Kass and P. Hoffer, Pulsed ESR studies of graphite intercalation compounds, *Synth.Met.* 23 (1988) 291-295.
18. S. Shimamura, A model for c-axis electrical conduction in graphite intercalation compounds, *Synth. Met.* 12 (1985) 365-370.